From Large 12-Membered Macrometallacycles to Ionic (NHC)₂M⁺Cl⁻ Type Complexes of Gold and Silver by Modulation of the *N*-Substituent of Amido-Functionalized N-Heterocyclic Carbene (NHC) Ligands

Manoja K. Samantaray,[†] Keliang Pang,[‡] Mobin M. Shaikh,[§] and Prasenjit Ghosh*,[†]

Department of Chemistry and National Single Crystal X-ray Diffraction Facility, Indian Institute of Technology, Bombay, Powai, Mumbai 400 076, and Department of Chemistry, Columbia University, 3000 Broadway, New York, New York 10027

A series of structurally diverse gold and silver complexes extending from ionic (NHC)₂M⁺Cl⁻ (M = Au, Ag) type complexes to large 12-membered macrometallacycles have been prepared by the appropriate modification of the *N*-substituent of amido-functionalized N-heterocyclic carbenes. Specifically, the ionic, [1-(R)-3-{*N*-(t-butylacetamido)imidazol-2-ylidene}]₂M⁺Cl⁻, (R = *t*-Bu, *i*-Pr; M = Au, Ag; **1b**, **1c**, **2b**, **2c**) complexes, were obtained in case of the N-*t*-butyl substituent of the amido-functionalized sidearm while 12-membered macrometallacycles, [1-(R)-3-{*N*-(2,6-di*i*-propylphenylacetamido)imidazol-2-ylidene}]₂M₂, (R = *t*-Bu, *i*-Pr; M = Au, Ag; **3b**, **3c**, **4b**, **4c**) were obtained in case of the 2,6-di*i*-propylphenyl *N*-substituent. These structurally diverse complexes of gold and silver were, however, prepared employing a common synthetic pathway involving the reactions of the imidazolium chloride salts (**1a**, **2a**, **3a**, **4a**) with Ag₂O to give the silver complexes (**1b**, **2b**, **3b**, **4b**) and which, when treated with (SMe₂)AuCl, gave the gold complexes (**1c**, **2c**, **3c**, **4c**). Detailed density functional theory studies of **1b**, **1c**, **2b**, **2c**, **3b**, **3c**, **4b**, and **4c** were carried out to gain insight about the structure, bonding, and the electronic properties of these complexes. The NHC−metal interaction in the ionic **1b**, **1c**, **2b**, and **2c** complexes is primarily composed of the interaction of the carbene lone pair with the empty p orbital of the metal (5p for Ag and 6p for Au) while the same in the macrometallacyclic **3b**, **3c**, **4b**, and **4c** complexes consisted of the interaction of the carbene lone pair with the empty s orbital of the metal (5s for Ag and 6s for Au). The observation of a low energy emission in about the 580–650 nm region has been tentatively assigned to originate from the presence of weak metallophilic interaction in these macrometallacyclic **3b**, **3c**, **4b**, and **4c** complexes.

Introduction

An interesting aspect of the silver(I) and gold(I) N-heterocyclic carbene chemistry is its structural diversity in the solid state, which displays a fascinating array of motifs ranging from a polymeric ladder,[1] to H-shaped structures,[2] to helical structures,[3,4] to rings,[5,4,6–8] to clusters,[9] and so forth, many of which are of considerable interest from the perspectives of materials, microelectronics, pharmaceuticals, and optoelectronic applications.[10,11] Both silver(I) and gold(I), which are renowned for their respective closed shell d¹⁰···d¹⁰ "argentophilic"[12] and "aurophilic" interactions,[13]

* To whom correspondence should be addressed. E-mail: pghosh@chem.iitb.ac.in. Fax: +91-22-2572-3480.
† Department of Chemistry, Indian Institute of Technology.
‡ Columbia University.
§ National Single Crystal X-ray Diffraction Facility, Indian Institute of Technology.

(1) (a) Qin, D.; Zeng, X.; Li, Q.; Xu, F.; Song, H.; Zhang, Z.-Z. *Chem. Commun.* **2007**, 147–149. (b) Lee, K. M.; Wang, H. M. J.; Lin, I. J. B. *J. Chem. Soc., Dalton Trans.* **2002**, 2852–2856.
(2) Lee, C. K.; Lee, K. M.; Lin, I. J. B. *Organometallics* **2002**, *21*, 10–12.
(3) Catalana, V. J.; Malwitz, M. A.; Etogo, A. O. *Inorg. Chem.* **2004**, *43*, 5714–5724.
(4) Chiu, P. L.; Chen, C. Y.; Lee, C.-C.; Hsieh, M.-H.; Chuang, C.-H.; Lee, H. M. *Inorg. Chem.* **2006**, *45*, 2520–2530.
(5) Larsen, A. O.; Leu, W.; Oberhuber, C. N.; Campbell, J. E.; Hoveyda, A. H. *J. Am. Chem. Soc.* **2004**, *126*, 11130–11131.
(6) Wanniarachchi, Y. A.; Khan, M. A.; Slaughter, L. M. *Organometallics* **2004**, *23*, 5881–5884.
(7) Legault, C. Y.; Kendall, C.; Charette, A. B. *Chem. Commun.* **2005**, 3826–3828.
(8) Catalano, V. J.; Moore, A. L. *Inorg. Chem.* **2005**, *44*, 6558–6566.
(9) (a) Zhou, Y.; Chen, W. *Organometallics* **2007**, *26*, 2742–2746. (b) Garrison, J. C.; Simons, R. S.; Kofron, W. G.; Tessier, C. A.; Youngs, W. J. *Chem. Commun.* **2001**, 1780–1781.

respectively, and also for their ability to bind to N and S donor ligands, thus provide an ideal platform for developing such engineered architectures.[14,15] Furthermore, of the many structurally characterized silver(I) and gold(I) complexes of N-heterocyclic carbenes that exist, examples of dinuclear ring type macrometallacyclic structures are relatively rare.[10,11] Though "self-assembly" remains a popular method for generating interesting extended frameworks, suitable control of the self-assembled structures still remains its primary challenge which, to some extent, has been alleviated by the proper choice of ligand, metal ion, solvent, template, counterion, and so forth.[16] Thus, the controlled synthesis of interesting motifs is of prime importance in this area of research.

Another important aspect of the silver(I) and gold(I) N-heterocyclic carbene complexes is their remarkable air, moisture, and thermal stability.[3,7,17–19] In this regard, we have recently reported several silver(I) complexes of N/O-functionalized N-heterocyclic carbenes that showed extremely high decomposition temperatures (ca. > 180 °C), for example, [(1-i-propyl-3-{N-phenylacetamido}imidazol-2-ylidene)$_2$Ag]$^+$Cl^{-18} and {[1-(2,4,6-trimethylphenyl)-3-(N-
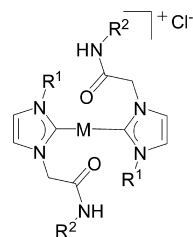
R^1 = i-Pr, R^2 = t-Bu, M = Ag (**1b**)
R^1 = i-Pr, R^2 = t-Bu, M = Au (**1c**)
R^1 = R^2 = t-Bu, M = Ag (**2b**)
R^1 = R^2 = t-Bu, M = Au (**2c**)
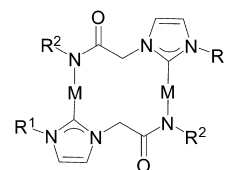
R^1 = i-Pr, R^2 = 2,6-i-Pr$_2$C$_6$H$_3$, M = Ag (**3b**)
R^1 = i-Pr, R^2 = 2,6-i-Pr$_2$C$_6$H$_3$, M = Au (**3c**)
R^1 = t-Bu, R^2 = 2,6-i-Pr$_2$C$_6$H$_3$, M = Ag (**4b**)
R^1 = t-Bu, R^2 = 2,6-i-Pr$_2$C$_6$H$_3$, M = Au (**4c**)

Figure 1

phenylacetamido)imidazol-2-ylidene]$_2$Ag}$^+$Cl^{-}.[19] Because of their greater stability, simpler synthetic route, and structural diversity, the gold and silver complexes are the preferred building blocks for materials application oriented research.

Our interest revolves around the design and utility of transition metal complexes of nonfunctionalized and N/O-functionalized N-heterocyclic carbenes in biomedical applications[20] and in chemical catalysis that range from their use in synthesizing biodegradable polylactide polymers[18,19,21] to C–C cross-coupling reactions.[22] During the course of the study we became interested in exploring the influence of the functionalized sidearm particularly on the structural diversity of the silver(I) and gold(I) complexes of N/O-functionalized N-heterocyclic carbenes. We envisioned that the functionalized sidearm may engage in chelation to a metal center, bridge between two metal centers, or participate in inter and intramolecular hydrogen bonding interactions thereby opening up possibilities for a variety of interesting structural motifs. We rationalized that a better understanding of the binding aspects of the functionalized sidearm followed by the modulation of its substituent would thus provide a better handle over systematic generation of structurally diverse motifs using the N/O-functionalized N-heterocyclic carbenes. We are also interested in knowing about the bonding and photophysical properties of these complexes.

In this contribution, we report a series of structurally diverse gold and silver complexes ranging from ionic (NHC)$_2$M$^+$Cl$^-$ (M = Au, Ag) type complexes (**1b**, **1c**, **2b**, **2c**) to large 12-membered macrometallacycles (**3b**, **3c**, **4b**, **4c**) (Figure 1), prepared by varying the N-substituent of the amido-functionalized sidearm from a t-butyl to a 2,6-di$i$-propylphenyl moiety. More importantly, since these diverse motifs were prepared by following a common synthetic route, the observed structural diversity can thus be envisioned as a direct consequence of the variation of the N-substituent of the amido-functionalized sidearm (Scheme 1). Apart from the synthetic studies, we report detailed density functional theory (DFT) studies that reflect on the nature of the NHC-

(10) (a) Kascatan-Nebioglu, A.; Panzner, M. J.; Tessier, C. A.; Cannon, C. L.; Youngs, W. J. *Coord. Chem. Rev.* **2007**, *251*, 884–895. (b) Lin, I. J. B.; Vasam, C. S. *Coord. Chem. Rev.* **2007**, *251*, 642–670. (c) Garrison, J. C.; Youngs, W. J. *Chem. Rev.* **2005**, *105*, 3978–4008. (d) Lin, I. J. B.; Vasam, C. S. *Comments Inorg. Chem.* **2004**, *25*, 75–129.

(11) Lin, I. J. B.; Vasam, C. S. *Can. J. Chem.* **2005**, *83*, 812–825.

(12) (a) Liu, X.; Guo, G.-C.; Fu, M.-L.; Liu, X.-H.; Wang, M.-S.; Huang, J.-S. *Inorg. Chem.* **2006**, *45*, 3679–3685. (b) Chi, Y.-N.; Huang, K.-L.; Cui, F.-Y.; Xu, Y.-Q.; Hu, C.-W. *Inorg. Chem.* **2006**, *45*, 10605–10612. (c) Wang, Q.-M.; Mak, T. C. W. *Inorg. Chem.* **2003**, *42*, 1637–1643. (d) Che, C.-M.; Tse, M.-C.; Chan, M. C. W.; Cheung, K.-K.; Phillips, D. L.; Leung, K.-H. *J. Am. Chem. Soc.* **2000**, *122*, 2464–2468.

(13) (a) Omary, M. A.; Mohamed, A. A.; Rawashdeh-Omary, M. A.; Frekler Jr., J. P. *Coord. Chem. Rev.* **2005**, *251*, 1372–1381. (b) Pyykkö, P. *Angew. Chem., Int. Ed.* **2004**, *43*, 4412–4456. (c) Gimeno, M. C.; Laguna, A. *Chem. Rev.* **1997**, *97*, 511–522. (d) Pyykkö, P. *Chem. Rev.* **1997**, *97*, 597–636. (e) Schmidbaur, H. *Chem. Soc. Rev.* **1995**, *24*, 391–400.

(14) (a) Gorin, D. J.; Toste, F. D. *Nature* **2007**, *446*, 395–403. (b) Hashmi, A. S. K.; Hutchings, G. J. *Angew. Chem., Int. Ed.* **2006**, *45*, 7896–7936. (c) Hoffmann-Röder, A.; Krause, N. *Org. Biomol. Chem.* **2005**, *3*, 387–391. (d) Puddephatt, R. J. *Coord. Chem. Rev.* **2001**, *216–217*, 313–332. (e) Vogler, A.; Kunkely, H. *Coord. Chem. Rev.* **2001**, *219–221*, 489–507. (f) Yam, V. W.-W.; Chan, C.-L.; Li, C.-K.; Wong, K. M.-C. *Coord. Chem. Rev.* **2001**, *216–217*, 173–194. (g) Laguna, A.; Laguna, M. *Coord. Chem. Rev.* **1999**, *193–195*, 837–856.

(15) (a) Zheng, S.-L.; Tong, M.-L.; Chen, X.-M. *Coord. Chem. Rev.* **2003**, *246*, 185–202. (b) Khlobystov, A. N.; Blake, A. J.; Champness, N. R.; Lemenovskii, D. A.; Majouga, A. G.; Zyk, N. V.; Schröder, M. *Coord. Chem. Rev.* **2001**, *222*, 155–192. (c) Munakata, M.; Wu, L. P.; Ning, G. L. *Coord. Chem. Rev.* **2000**, *198*, 171–203.

(16) (a) Huang, W.; Zhu, H.-B.; Gou, S.-H. *Coord. Chem. Rev.* **2006**, *250*, 414–423. (b) Piguet, C.; Borkovec, M.; Hamacek, J.; Zeckert, K. *Coord. Chem. Rev.* **2005**, *249*, 705–726. (c) Hoeben, F. J. M.; Jonkheijm, P.; Meijer, E. W.; Schenning, A. P. H. J. *Chem. Rev.* **2005**, *105*, 1491–1546. (d) Swiegers, G. F.; Malefetse, T. J. *Chem. Rev.* **2000**, *100*, 3483–3537.

(17) (a) Wang, J.-W.; Li, Q.-S.; Xu, F.-B.; Song, H.-B.; Zhang, Z.-Z. *Eur. J. Org. Chem.* **2006**, *130*, 1301–1316. (b) Hu, X.; Castro-Rodriguez, I.; Olsen, K.; Meyer, K. *Organometallics* **2004**, *23*, 755–764. (c) Hu, X.; Tang, Y.; Gantzel, P.; Meyer, K. *Organometallics* **2003**, *22*, 612–614. (d) Liu, Q.-X.; Xu, F.-B.; Li, Q.-S.; Zeng, X.-S.; Leng, X.-B.; Chou, Y. L.; Zhang, Z.-Z. *Organometallics* **2003**, *22*, 309–314.

(18) Samantaray, M. K.; Katiyar, V.; Pang, K.; Roy, D.; Nanavati, H.; Stephen, R.; Sunoj, R. B.; Ghosh, P. *Eur. J. Inorg. Chem.* **2006**, 2975–2984.

(19) Samantaray, M. K.; Katiyar, V.; Pang, K.; Nanavati, H.; Ghosh, P. *J. Organomet. Chem.* **2007**, *692*, 1672–1682.

(20) Ray, S.; Mohan, R.; Singh, J. K.; Samantaray, M. K.; Shaikh, M. M.; Panda, D.; Ghosh, P. *J. Am. Chem. Soc.* **2007**, *129*, 15042–15053.

(21) (a) Ray, L.; Katiyar, V.; Barman, S.; Raihan, M. J.; Nanavati, H.; Shaikh, M. M.; Ghosh, P. *J. Organomet. Chem.* **2007**, *692*, 4259–4269. (b) Ray, L.; Katiyar, V.; Raihan, M. J.; Nanavati, H.; Shaikh, M. M.; Ghosh, P. *Eur. J. Inorg. Chem.* **2006**, 3724–3730.

(22) (a) Ray, L.; Shaikh, M. M.; Ghosh, P. *Dalton Trans.* **2007**, 4546–4555. (b) Ray, L.; Shaikh, M. M.; Ghosh, P. *Organometallics* **2007**, *26*, 958–964.

Scheme 1

metal interactions present in these complexes. In addition, the photoluminescence studies, carried out to probe the presence of the closed shell M···M (M = Ag, Au) interaction in these complexes, are also reported.

Results and Discussion

Of the many different shapes and sizes that have been observed in the silver(I)−NHC and also, to some extent, in the gold(I)-NHC complexes, the ring structures, particularly the large macrometallacyclic ones, are surprisingly few.[10,11] We are aware of only a handful of structurally characterized examples of macrometallacycles of silver(I), namely, the 16-membered [1-(mesityl)-3-{(naphthalen-1-yl)naphthalen-2-ol} imidazolin-2-ylidene]₂Ag₂,[5] the 14 membered {[1-(naphthalen-2-ylmethyl)-3-(3,5-dimethyl-1-ethylpyrazole)imidazol-2-ylidene]₂Ag₂}2(NO₃)[4] and {[1-(4-fluorobenzyl)-3-(3,5-dimethyl-1-ethylpyrazole)imidazol-2-ylidene]₂Ag₂}2-(NO₃),[4] the 12-membered {[methylene-*bis*(3-mesityl)imidazol-2-ylidene]₂Ag₂}2(BF₄),[6] and the 8-membered [1-(benzamide)-3-(mesityl)imidazol-2-ylidene]₂Ag₂[7] complex, and of a single report of a structurally characterized 12-membered gold complex, {[1-(pyridyl-2-ylmethyl)-3-(methyl)imidazol-2-ylidene}₂Au₂]2(BF₄).[8] Thus, synthetic routes leading to stable ring structures like large macrometallacycles remain a challenge and are highly desirable. Our present effort details the use of a simple common synthetic methodology for preparing families of ionic (NHC)₂M⁺Cl⁻ (M = Au, Ag) type complexes and large 12-membered macrometallacycles of silver(I) and gold(I) supported over amido-functionalized N-heterocyclic carbenes by sheer modulation of the N-substituent from a *t*-butyl to a 2,6-di*i*-propylphenyl moiety of a functionalized sidearm of the carbene ligand (Scheme 1).

Ionic (NHC)₂M⁺Cl⁻ (M = Au, Ag) Type Complexes. The amido-functionalized N-heterocyclic carbene ligand precursors, 1-(R)-3-{*N*-(t-butylacetamido)}imidazolium chloride (R = *t*-Bu, *i*-Pr; **1a**, **2a**), bearing a *t*-butylacetamido

sidearm, were synthesized by the direct alkylations of 1-*i*-propylimidazole and 1-*t*-butylimidazole with *N*-*t*-butylchloroacetamide in 72 and 75% yields, respectively.

The reactions of the imidazolium chloride salts, **1a** and **2a**, with Ag₂O gave the ionic [1-(R)-3-{*N*-(t-butylacetamido)imidazol-2-ylidene}]₂Ag⁺Cl⁻, (R = *t*-Bu, *i*-Pr; **1b**, **2b**) complexes. Quite interestingly, the amido resonance -CON*H*(*t*-Bu) appeared at 7.65 ppm (**1b**) and at 8.34 ppm (**2b**), at values that are significantly downfield shifted by about 1.5–2.0 ppm from that of *N*-*t*-butylchloroacetamide (6.32 ppm), thereby suggesting the presence of a strong [Cl···H−N] type hydrogen bonding interaction in solution between the Cl⁻ anion and the amide-N*H* proton of the *N*-*t*-butylacetamido sidearm.

The definitive proof of the hydrogen bonding interaction between the Cl⁻ anion and the amide-N*H* protons of the *N*-*t*-butylacetamido sidearms came from the molecular structures of **1b** and **2b** (Table 1, Figure 2 and Supporting Information, Figure S1) that showed two close Cl···N distances [3.254 Å (**1b**), 3.243 Å (**2b**)], which were shorter than the sum of the individual van der Waals radii of Cl and N (3.30 Å).[23] An important outcome of the hydrogen bonding interaction was the *cis* orientation of the two *N*-*t*-butylacetamido sidearms in **1b** and **2b** that occurred because of an interaction of the centrally located Cl⁻ anion with the amide-N*H* protons of the two *N*-*t*-butylacetamido sidearms resulting in an interesting [N−H···Cl···H−N] type hydrogen bonding interaction. Another interesting consequence of the hydrogen bonding was the observed noncoplanarity of the two *trans* imidazole rings in **1b** and **2b** with the dihedral angle [∠ N2−C1−Ag1−C1−N1] between the imidazole rings being 122.9 ° (**1b**) and 123.2° (**2b**). In this context, it is worth mentioning that in ionic (NHC)₂Ag⁺Cl⁻ type complexes, both structures, that is, the ones with coplanar imidazole rings as well as the ones in which they are noncoplanar, are often

---

(23) Bondi, A. *J. Phys. Chem.* **1964**, *68*, 441–451.
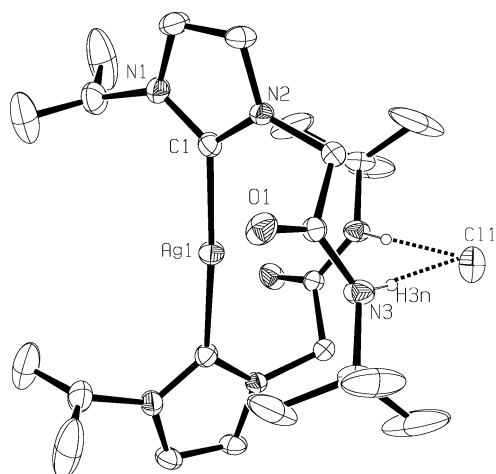
Figure 2. ORTEP (Oak Ridge thermal ellipsoid plot) of **1b** with thermal ellipsoids drawn at 20% probability level. Selected bond lengths (Å) and angles (°): N1−C1 1.335(5), N2−C1 1.346(5), Ag1−C1 2.087(4), C1−Ag1−C1 176.6(2), N1−C1−N2 105.0(3).

Figure 3. ORTEP of **1c** with thermal ellipsoids drawn at 20% probability level. Selected bond lengths (Å) and angles (°): N1−C1 1.332(9), N2−C1 1.357(9), Au1−C1 2.017(7), C1−Au1−C1 178.3(4), N1−C1−N2 105.1(6).

observed. For example, in {[1-(2,4,6-trimethylphenyl)-3-(N-phenylacetamido)imidazol-2-ylidene]_2Ag}^+Cl^-,[19] the *trans* imidazole rings were found to be noncoplanar while those in {[(1-*i*-propyl)-3-{N-phenylacetamido}imidazol-2-ylidene)]_2Ag}^+Cl^-[18] were coplanar. It is worth noting that the computational studies carried out by us[18] showed that for {[(1-*i*-propyl)-3-{N-phenylacetamido}imidazol-2-ylidene)]_2Ag}^+Cl^-, the noncoplanar structure was found to be more stable by 2.66 kcal/mol in the gas phase over the coplanar structure as a result of an intramolecular hydrogen bonding interaction.

The Ag−C_{carb} bond distances in **1b** [2.087(4) Å] and in **2b** [2.0912(17) Å] are significantly shorter than the sum of individual covalent radii of Ag and C (2.111 Å)[24] and are comparable to those in other reported silver(I)−NHC complexes.[18,19,21] The angle at silver is linear in **1b** [∠ C1−Ag1−C1 = 176.5(2)°] and in **2b** [∠ C1−Ag−C1 = 178.18(9)°] complexes.

The treatment of the silver **1b** and **2b** complexes with (SMe_2)AuCl gave the corresponding ionic, [1-(R)-3-{N-(t-butylacetamido)imidazol-2-ylidene}]_2Au^+Cl^-, (R = *t*-Bu, *i*-Pr; **1c**, **2c**), complexes. As was observed in the case of the silver counterparts, indications of [Cl···H−N] type hydrogen bonding interactions in solution between the Cl^- anion and the amide-N*H* protons of the *N-t*-butylacetamido sidearms were very much seen in these gold **1c** and **2c** complexes too, as the amido resonance −CON*H*(t-Bu) appeared significantly shifted to 8.90 ppm (**1c**) and 8.84 ppm (**2c**), again, relative to that of *N-t*-butylchloroacetamide (6.32 ppm) in the ^1H NMR spectrum.

Indeed, the molecular structures of the gold **1c** and **2c** complexes (Table 1, Figure 3 and Supporting Information, Figure S2) showed the presence of [N−H···Cl···H−N] type hydrogen bonding interactions analogous to that observed in the case of the silver **1b** and **2b** complexes resulting in the *cis* orientations of the two *N-t*-butylacetamido sidearms in the **1c** and **2c** complexes. The Cl···N distances, each of
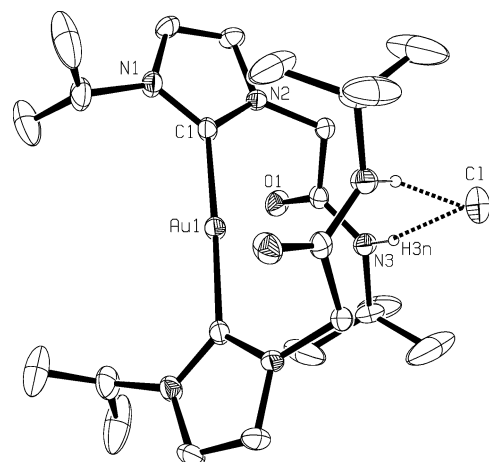
3.261 Å (**1c**) and of 3.243 Å (**2c**), are also comparable to what was observed in the silver **1b** (3.254 Å) and **2b** (3.243 Å) complexes. Consistent with the smaller covalent radii of Au compared to Ag [r(Au) = 1.25 Å and r(Ag) = 1.33 Å in the two-coordinate environment],[25] the Au−C_{carb} distances in **1c** [2.017(7) Å] and **2c** [2.028(5) Å] are indeed shorter than the Ag−C_{carb} distances in **1b** [2.087(4) Å] and **2b** [2.0912(17) Å]. The gold **1c** and **2c** complexes are isostructural with the silver **1b** and **2b** complexes. The *trans* imidazole rings displayed nonplanar orientations in these gold complexes.

12-Membered Macrometallacyclic (NHC)_2M_2 (M = Ag, Au) Complexes. The large 12-membered macrometallacyclic [1-(R)-3-{N-(2,6-di*i*-propylphenylacetamido)imidazol-2-ylidene}]_2M_2, (R = *t*-Bu, *i*-Pr; M = Au, Ag; **3b**, **3c**, **4b**, **4c**) complexes were synthesized employing the same synthetic methodology as applied for synthesizing the ionic **1b**, **1c**, **2b**, and **2c** complexes. It is worth noting that these neutral 12-membered macrometallacyclic **3b**, **3c**, **4b**, and **4c** complexes possessed a 2,6-di*i*-propylphenyl moiety as the N-substituent of the amido-functionalized sidearm of the N-heterocyclic carbene ligand instead of the *t*-butyl N-substituent present in case of the ionic **1b**, **1c**, **2b**, **2c** complexes. Specifically, the 1-(R)-3-{N-(2,6-di*i*-propylphenylacetamido)imidazolium chloride salts (R = *t*-Bu, *i*-Pr; **3a**, **4a**), bearing 2,6-di*i*-propylphenylacetamido sidearms, were synthesized by the direct alkylation of the respective imidazoles with *N*-2,6-di*i*-propylphenylchloroacetamide in 79% yields. The amido-N*H* resonance in **3a** and **4a** was identified by D_2O exchange studies using ^1H NMR spectroscopy.

The silver complexes [1-(R)-3-{N-(2,6-di*i*-propylphenylacetamido)imidazol-2-ylidene}]_2Ag_2, (R = *t*-Bu, *i*-Pr; **3b**, **4b**) were obtained from the reaction of the imidazolium chloride salts **3a** and **4a** with Ag_2O. Quite interestingly, the ^1H NMR spectrum of **3b** and **4b** showed not only the expected absence of a downfield peak, owing to the deprotonation of the NC*H*N proton of the reactant imidazolium chloride salts, but

(24) Pauling, L. *The Nature of the Chemical Bond*, 3rd ed.; Cornell University Press: Ithaca, NY, 1960; p 224−228, 256−258.

(25) Tripathi, U. M.; Bauer, A.; Schmidbaur, H. *J. Chem. Soc., Dalton Trans.* **1997**, 2865−2868.

Table 1. X-ray Crystallographic Data for **1b**, **1c**, **2b**, and **2c**

compound	1b	1c	2b	2c
lattice	monoclinic	monoclinic	monoclinic	monoclinic
formula	$C_{24}H_{42}AgClN_6O_2$	$C_{24}H_{42}AuClN_6O_2$	$C_{26}H_{46}AgClN_6O_2$	$C_{26}H_{46}AuClN_6O_2$
formula weight	589.96	679.05	618.01	707.10
space group	*C2/c*	*C2/c*	*C2/c*	*C2/c*
a, Å	14.8308(7)	14.7600(13)	15.0315(6)	15.0040(6)
b, Å	15.3548(11)	15.425(3)	16.2804(6)	16.4270(7)
c, Å	13.3109(8)	13.2705(10)	12.5493(5)	12.5535(7)
α, °	90.00	90.00	90.00	90.00
β, °	93.132(5)	94.175(7)	93.5880(10)	94.669(4)
γ, °	90.00	90.00	90.00	90.00
V, Å³	3026.7(3)	3013.4(6)	3065.0(2)	3083.8(2)
Z	4	4	4	4
temperature (K)	293(2)	293(2)	243(2)	120(2)
radiation (λ, Å)	0.71073	0.71073	0.71073	0.71073
ρ(calcd.), g cm⁻³	1.295	1.497	1.339	1.523
μ(Mo Kα), mm⁻¹	0.783	4.999	0.776	4.889
θ max, deg.	27.46	27.46	28.37	30.00
no. of data	3472	3446	3617	4488
no. of parameters	164	164	195	170
R_1	0.0487	0.0509	0.0264	0.0415
wR_2	0.1044	0.1143	0.0702	0.0861
GOF	1.034	1.036	1.040	0.921

also the absence of the amide(N*H*) proton of the *N*-2,6-di*i*-propylphenylacetamido sidearm suggesting its deprotonation by Ag₂O. Thus, the deprotonations of the NC*H*N and the amide(N*H*) protons of the imidazolium chloride salts **3a** and **4a** when treated with Ag₂O are in sharp contrast to what was observed in the formation of the ionic **1b** and **2b** complexes, where only the deprotonation of the NC*H*N proton of the imidazolium chloride salts **1a** and **2a** was seen to occur under analogous conditions. The observed difference of the amide(N*H*) proton reactivity is consistent with its more acidic nature when the N-substituent is a 2,6-di*i*-propylphenyl moiety as in **3a** and **4a** as opposed to a *t*-butyl moiety as in **1a** and **2a**, thereby resulting in its deprotonation in former case.

The simultaneous deprotonations of the NC*H*N and the amide(N*H*) protons of the imidazolium chloride salts **3a** and **4a**, when treated with Ag₂O, had a significant impact on the respective geometries as their molecular structures revealed the formation of neutral 12-membered macrometallacycles of the type [1-(R)-3-{*N*-(2,6-di*i*-propylphenylacetamido)imi-dazol-2-ylidene}]₂Ag₂, (R = *t*-Bu, *i*-Pr; **3b**, **4b**; Figures 4, 5, and Supporting Information, Figure S3). These silver macrometallacycles were formed by head-to-tail arrangements of two [1-(R)-3-{*N*-(2,6-di*i*-propylphenylacetami-do)imidazol-2-ylidene}] fragments conjoined by two bridging Ag atoms. The geometries around the silver centers were off-linear with the angles at the silver being 171.6(2)° (∠ C1−Ag1−N3; **3b**) and 170.31(14)° (∠ C1−Ag1−N6; **4b**). The Ag−C_carb distance in the neutral **3b** [2.066(8) Å] and **4b**

[2.032(4) Å and 2.045(4) Å] complexes was slightly shorter than that observed in the related cationic **1b** [2.087(4) Å] and **2b** [2.0912(17) Å] complexes. The Ag−N bond distance was 2.084(6) Å in **3b**, 2.073(3) Å and 2.062(3) Å in **4b**, and was slightly longer than the sum of the individual covalent radii of Ag and N (2.04 Å).[24]

An important structural feature of these 12-membered macrometallacycles is its ring conformation (Figure 4). Quite interestingly, the *chair* conformation was seen in the unit cell of **3b** while both the *chair* and the *boat* conformations were observed in that of **4b** (Table 2, Supporting Information, Figure S3). The 12-membered macrometallacycles were formed by head-to-tail arrangements of the amido-function-alized sidearm, the imidazole carbene, and the silver atom. The Ag···Ag distances of 3.403 Å (*chair*) and 3.550 Å (*chair*) were observed in **3b**, and those of 3.771 Å (*chair*) and 3.505 Å (*boat*) were observed in the **4b** complex. Quite interestingly, the low temperature ¹H NMR spectrum of **4b** recorded at –40 °C showed a single set of resonances similar to that of its room temperature spectrum suggesting rapid

boat conformation   *chair* conformation
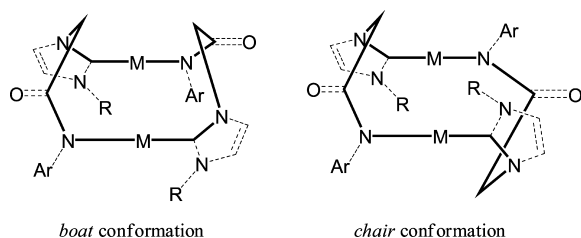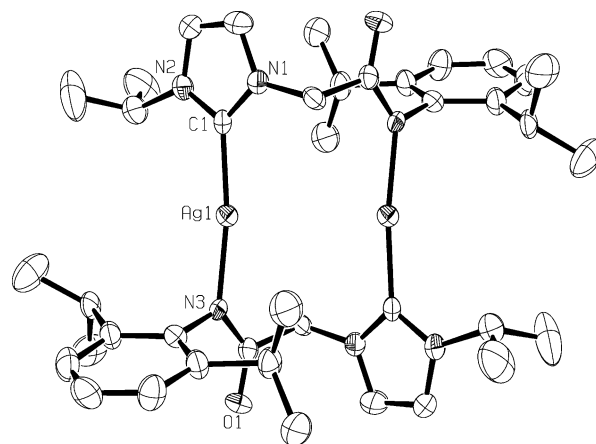
Figure 4

Figure 5. ORTEP of **3b** with thermal ellipsoids drawn at 50% probability level. Selected bond lengths (Å) and angles (°): Ag1−C1 2.066(8), Ag1−N3 2.084(6), N1−C1 1.344(9), N2−C1 1.347(9), C1−Ag1−N3 171.6(2), N1−C1−N2 104.5(7). The *chair* conformation is shown.

exchange between the two conformations. The flag pole-flag pole distance, as defined by the methylene carbon-methylene carbon [(CH_2)···(CH_2)] contact, is 5.093 Å in the *boat* conformation of **4b,** whereas the same is slightly elongated at 5.587 Å in the *chair* conformation of **4b**. The similar methylene carbon−methylene carbon [(CH_2)···(CH_2)] contact is slightly longer at 5.922 Å and 5.845 Å in the *chair* conformation of **3b**.

Interestingly enough, several different conformations have been reported for the structurally characterized macromet-allacycles of silver−NHC complexes. For example, a 12-membered macrometallacycle, {[methylene-*bis*(3-mesityl)-imidazol-2-ylidene]$_2$Ag$_2$}2(BF$_4$),[6] displayed a twisted-boat conformation while the much smaller 8-membered macrometallacycle, [1-(benzamide)-3-(mesityl)imidazol-2-ylidene]$_2$-Ag$_2$,[7] exhibited a flat planar structure with a strong argentophilic interaction as evident from a short Ag···Ag contact of 2.782 Å.

The gold complexes [1-(R)-3-{*N*-(2,6-di*i*-propylphenylac-etamido)imidazol-2-ylidene}]$_2$Au$_2$, (R = *t*-Bu, *i*-Pr; **3c**, **4c**) were conveniently synthesized from their silver analogs **3b** and **4b** by the treatment with (SMe$_2$)AuCl. Both the ^{1}H NMR and the ^{13}C{^{1}H} NMR spectrum of the gold **3c** and **4c** complexes closely resembled those of the silver **3b** and **4b** complexes, suggesting that earlier observed 12-membered macrometallacyclic structures are retained in the case of the gold complexes too. Indeed, high resolution electrospray mass spectrum (HRMS) of **3c** showed a peak at *m/z* 1047.3907, corresponding to the cationic {[1-(*i*-propyl)-3-{*N*-(2,6-di*i*-propylphenylacetamido)imidazol-2-ylidene}]$_2$Au$_2$}[+] species (calculated *m/z* 1047.3874), and that of **4c** at *m/z* 1075.4143, corresponding to the cationic {[1-(*t*-butyl)-3-{*N*-(2,6-di*i*-pro-pylphenylacetamido)imidazol-2-ylidene}]$_2$Au$_2$}[+] species (calculated *m/z* 1075.4187). Interestingly enough, the HRMS data indicate that the 12-membered macrometallacyclic structure of the gold **3c** and **4c** complexes is maintained in solution under mass spectrometry sampling conditions and thus point toward the high stabilities of these ring structures.

Indeed, the molecular structure of the gold **3c** and **4c** complexes (Table 2, Figure 6 and Supporting Information, Figure S4) showed analogous 12-membered macrometalla-cyclic motifs observed in the case of the silver **3b** and **4b** complexes. Furthermore, similar to what was seen in the silver **3b** and **4b** structures, two conformations, the *boat* and the *chair* forms, were also observed in the gold **3c** and **4c** complexes. For example, the unit cell of **3c** contained the *chair* conformation while that of the **4c** contained both the *boat* and the *chair* conformations. The Au···Au separations were 3.985 Å (*chair*) in **3c**, 3.899 Å (*chair*) and 3.649 Å (*boat*) in **4c**, and are greater than twice the van der Waals radii of Au (3.32 Å).[23] It is worth noting that the ^{1}H NMR data of **4c** recorded at room temperature and at −40 °C suggested a rapid exchange between the *chair* and the *boat* conformations as evidenced by a single set of resonances observed at these temperatures.

Quite expectedly, the Au−C$_{carb}$ distances in **3c** [1.982(3) Å] and **4c** [1.989(3) Å, 1.990(3) Å] were shorter than the corresponding distances in the silver **3b** [2.066(8) Å] and
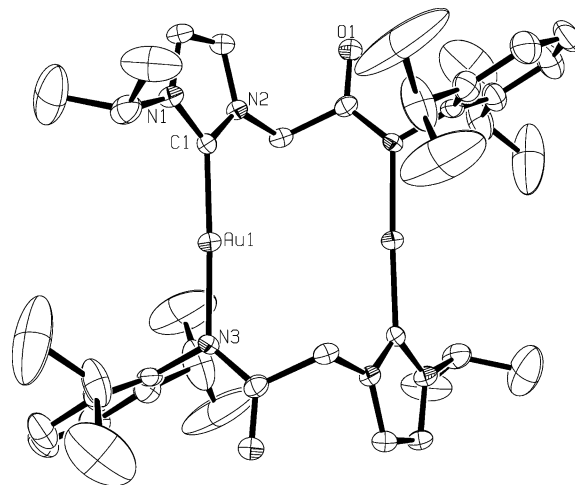
Figure 6. ORTEP of **3c** with thermal ellipsoids drawn at 50% probability level. Selected bond lengths (Å) and angles (°): N1−C1 1.354(4), N2−C1 1.357(5), Au1−C1 1.982(3), Au1−N3 2.037(3), N1−C1−N2 104.6(3), C1−Au1−N3 177.32(12). The *chair* conformation is shown.

4b [2.032(4) Å, 2.045(4) Å] complexes, owing to the smaller covalent radii of Au compared to Ag.[25] Notably, that the Au−C$_{carb}$ distances in the neutral **3c** [1.982(3) Å] and **4c** [1.989(3) Å and 1.990(3) Å] complexes are slightly shorter than in the related cationic **1c** [2.017(7) Å] and **2c** [2.028(5) Å] complexes. The angle at the gold atom is linear in the **3c** [∠ C1−Au1−N3 = 177.32(12)°] and **4c** [∠ C1−Au1−N6 = 172.86(13)°] complexes and is similar to that observed in the silver complexes (**3b** and **4b**).

It is worth comparing the **3c** and **4c** structures with other known related gold macrometallacycles; however, they are surprisingly sparse in comparison to the silver ones. For example, another structurally characterized 12-membered gold macrometallacyclic complex, {[1-(pyridyl-2-ylmethyl)-3-(methyl)imidazol-2-ylidene}$_2$Au$_2$]2(BF$_4$),[8] exhibited a twisted-boat conformation in the crystal lattice unlike the regular *chair* and *boat* conformations observed in the **3c** and **4c** structures. Quite interestingly, the Au···Au separation of 3.173 Å in the 12-membered {[1-(pyridyl-2-ylmethyl)-3-(methyl)imidazol-2-ylidene}$_2$Au$_2$]2(BF$_4$)[8] complex was significantly shorter than in the related 12-membered **3c** (3.985 Å) and **4c** (3.649 Å, 3.899 Å) macrometallacyles.

Density Functional Theory Studies. To gain a better understanding of nature of the chemical bonding, the structure, and the electronic properties, detailed density functional theory studies were carried out on these silver and gold complexes, **1b**, **1c**, **2b**, **2c**, **3b**, **3c**, **4b**, and **4c**. Specifically, single-point calculations on the **1b**, **1c**, **2b**, **2c**, **3b**, **3c**, **4b**, and **4c** complexes were performed at the B3LYP/SDD, 6–31G* level of theory using the atomic coordinates adopted from X-ray analysis.[26] In addition, similar calculations were performed on the respective free N-heterocyclic carbene ligands and on the metal ion(s) obtained after fragmenting each of the **1b**, **1c**, **2b**, **2c**, **3b**, **3c**, **4b**, and **4c**

(26) The single-point calculations performed on the X-ray structures of the 12-membered macrometallacyclic **3b**, **3c**, **4b**, and **4c** complexes were all of the *chair* conformations. It is worth noting that the *boat* conformation was, however, also found to exist alongside the *chair* conformation in the unit cell only in case of the **4b** and **4c** complexes.

Table 2. X-ray Crystallographic Data for **3b**, **3c**, **4b**, and **4c**

compound	3b	3c	4b	4c
lattice	monoclinic	monoclinic	triclinic	triclinic
formula	$C_{43}H_{58}Ag_2Cl_{10}N_6O_2$	$C_{20}H_{28}AuN_3O$	$C_{130}H_{186}Ag_6N_{20}O_6$	$C_{130}H_{186}Au_6N_{20}O_6$
formula weight	1261.19	523.42	2772.26	3306.79
space group	$P2_1/c$	$P2_1/c$	$P\bar{1}$	$P\bar{1}$
a, Å	21.2562(4)	10.840(2)	10.443(4)	10.4137(17)
b, Å	17.7215(3)	9.1945(18)	15.018(2)	14.9079(9)
c, Å	14.4660(3)	21.0125(12)	23.5459(17)	23.467(2)
α, °	90.00	90.00	103.069(9)	107.295(7)
β, °	94.245(2)	98.704(9)	101.016(15)	95.024(10)
γ, °	90.00	90.00	104.51(2)	104.362(9)
V, Å³	5434.27(18)	2070.1(6)	3360.1(15)	3318.1(6)
Z	4	4	1	1
temperature (K)	150(2)	150(2)	120(2)	150(2)
radiation (λ, Å)	0.71073	0.71073	0.71073	0.71073
ρ(calcd.), g cm⁻³	1.542	1.679	1.370	1.655
μ(Mo Kα), mm⁻¹	1.252	7.118	0.915	6.666
θ max, deg.	25.00	29.99	30.00	30.00
no. of data	9531	6004	19531	18958
no. of parameters	580	232	752	752
R_1	0.0678	0.0287	0.0488	0.0273
wR_2	0.1868	0.0618	0.0531	0.0538
GOF	1.082	0.989	0.817	1.096

complexes (Supporting Information, Figure S5). To asses the nature of the NHC—M (M = Ag, Au) interaction, the post-wave function analysis using the natural bond orbital (NBO) method[27] was performed on the **1b**, **1c**, **2b**, **2c**, **3b**, **3c**, **4b**, and **4c** complexes, their respective ligands, and the metal ion fragments (Supporting Information, Figure S5).

It is interesting to note that for the (NHC)₂M⁺Cl⁻ (M = Au, Ag) type **1b**, **1c**, **2b**, **2c** complexes, the Mulliken charge analyses (Supporting Information, Table S9) showed that as a result of electron donation [NHC → M (M = Ag, Au)] from the free NHC fragment to the metal center, the charge on the metal center in the **1b**, **1c**, **2b**, and **2c** complexes are significantly reduced compared to that of the free metal ions along with concomitant increase in charge on the NHC fragments in the respective **1b**, **1c**, **2b**, **2c** complexes relative to that of the free NHC ligands. It is worth noting that the 12-membered macrometallacyclic gold and silver complexes, **3b**, **3c**, **4b**, and **4c**, also showed a similar trend (Supporting Information, Table S10).

Indeed, the electronic configuration of the metal in the **1b** [$5s^{0.75}$, $4d^{9.78}$, $5d^{0.01}$, $6p^{0.01}$], **1c** [$6s^{1.03}$, $5d^{9.62}$, $6p^{0.01}$, $6d^{0.01}$, $7p^{0.01}$], **2b** [$5s^{0.71}$, $4d^{9.79}$, $5p^{0.01}$, $5d^{0.01}$], and **2c** [$6s^{1.01}$, $5d^{9.63}$, $6p^{0.01}$, $6d^{0.01}$, $7p^{0.01}$] complexes, when compared to the respective free ion [Ag⁺ ($5s^0$, $4d^{10}$), Au⁺ ($6s^0$, $5d^{10}$)] configuration, indicate that the maximum electron donation [NHC → M (M = Ag, Au)] from the free NHC fragment to the metal center occurred at the 5s (silver) and 6s (gold) orbitals (Supporting Information, Table S11). Accordingly, further NBO analysis revealed the NHC—M (M = Ag, Au) bond to be composed of an interaction between a hybrid C_{carb} (sp²) orbital with an sd hybrid metal orbital having predominantly s character, as can be seen in the **1b** [C(sp$^{1.65}$)−Ag(sd$^{0.12}$)], **1c** [C(sp$^{1.60}$)−Au(sd$^{0.26}$)], **2b** [C(sp$^{1.57}$)−Ag-(sd$^{0.11}$)], and **2c** [C(sp$^{1.65}$)−Au(sd$^{0.24}$)] complexes. Analogous NBO analysis of the electronic configurations of the 12-membered macrometallacyclic {(NHC)₂M₂} complexes re-

vealed similar electron donation occurring to the unfilled s orbital of the metal ion in the **3b**, **3c**, **4b**, and **4c** complexes (Supporting Information, Table S12).

To gauge the strength of the NHC−M (M = Ag, Au) interaction in these silver and gold complexes, the NHC−metal bond dissociation energies, D_e(NHC−M) (M = Ag, Au), of **1b**, **1c**, **2b**, **2c**, **3b**, **3c**, **4b**, and **4c** were computed using the B3LYP/SDD, 6–31G(d) level of theory (Supporting Information, Tables S13 and 14). Interestingly, the Au−NHC bond energies were found to be higher [**1c** 113.6 kcal/mol; **2c** 112.4 kcal/mol] than the Ag−NHC bond energies [**1b** 86.9 kcal/mol; **2b** 83.2 kcal/mol] and resemble the trend reported earlier by Frenking[28] for a variety of (NHC)MCl (M = Ag, Au) type complexes (Supporting Information, Table S13). The unusually strong Au−NHC bond strengths observed in gold complexes were attributed to be a consequence of the relativistic contraction of the 6s orbital.[14a] Furthermore, for **1c** and **2c**, being cationic {(NHC)₂Au}⁺Cl⁻ in nature, the Au−NHC bond energies [**1c** 113.6 kcal/mol; **2c** 112.4 kcal/mol] are even higher compared to those in the neutral (NHC)AuCl type complexes. For example, the Au−NHC bond dissociation energy for the simple unsubstituted neutral (imidazol-2-ylidene)AuCl complex has been estimated to be 82.8 kcal/mol.[28] A similar trend is also observed in silver complexes on going from cationic (NHC)₂Ag⁺Cl⁻ type **1b** and **2b** complexes [**1b** 86.9 kcal/mol; **2b** 83.2 kcal/mol] to neutral (NHC)AgCl type complexes like (imidazol-2-ylidene)AgCl [56.5 kcal/mol][28] and [1-*i*-propyl-3-(2-oxo-2-*t*-butyl ethyl)imidazol-2-ylidene]AgCl [50.8 kcal/mol].[29]

Quite interestingly, despite the fact that numerous silver and gold NHC complexes have been synthesized, structurally characterized, and employed in a variety of catalysis, as well

(27) Reed, A. E.; Curtiss, L. A.; Weinhold, F. *Chem. Rev.* **1988**, *88*, 899–926.

(28) (a) Nemcsok, D.; Wichmann, K.; Freenking, G. *Organometallics* **2004**, *23*, 3640–3646. (b) Boehme, C.; Frenking, G. *Organometallics* **1998**, *17*, 5801–5809.

(29) Samantaray, M. K.; Roy, D.; Patra, A.; Stephen, R.; Saikh, M.; Sunoj, R. B.; Ghosh, P. *J. Organomet. Chem.* **2006**, *691*, 3797–3805.

as in biomedical, applications, theoretical studies on these complexes remain surprisingly scarce, with a few reported by Meyer,[17b,c] Frenking,[28] and us.[18,29]

A direct relationship of the C_{carb}—M (M = Ag, Au) bond distances with the NHC—metal bond energies could be observed in the (NHC)$_2$M$^+$Cl$^-$ type silver and gold complexes, namely, the decrease in bond distance was accompanied by an increase in bond energy. For example, the NHC—metal bond distance ($d(C_{carb}$—M) and the NHC—metal bond dissociation energy D_e(NHC—M) in these silver, **1b** [2.087(4) Å, 86.9 kcal/mol], **2b** [2.0912(17) Å, 83.2 kcal/mol] and gold, **1c** [2.017(7) Å, 113.6 kcal/mol], **2c** [2.028(5) Å, 112.4 kcal/mol] complexes bear an inverse correlation (Supporting Information, Table S13). Consistent with the NHC ligand being less bulkier owing to the presence of an *i*-propyl N-substituent in the silver **1b** and gold **1c** complexes than that in the **2b** and **2c** complexes, containing a *t*-butyl N-substituent, the NHC—M bond distance in **1b** and **1c** are shorter than in **2b** and **2c**. However, for the 12-membered macrometallacyclic {(NHC)$_2$M$_2$} type complexes, **3b**, **3c**, **4b**, and **4c**, no such correlation of the NHC—M bond energies with the NHC—M bond distances were observed presumably because the NHC—M bond distance is more of a consequence of the macrometallacyclic geometry (Supporting Information, Table S14).

Lastly, the charge decomposition analysis (CDA) of **1b**, **1c**, **2b**, **2c**, **3b**, **3c**, **4b**, and **4c** was undertaken to obtain an estimate of the [NHC $\overset{\sigma}{\leftarrow}$ M] donation, designated by d, and the [NHC $\overset{\pi}{\leftarrow}$ M] backward donation, designated by b, occurring in these complexes. Interestingly, greater [NHC $\overset{\pi}{\leftarrow}$ M] backward donation is seen to occur in the gold **1c**, **2c**, **3c**, and **4c** complexes exhibiting lower (d/b) ratios of 5.23, 5.88, 5.58, and 5.63 respectively as compared to the silver **1b** (11.44), **2b** (12.53), **3b** (12.68), and **4b** (12.32) complexes (see Supporting Information, Tables S15 and S16). Similar greater [NHC $\overset{\pi}{\leftarrow}$ M] backward donation in Au—NHC complexes relative to Ag—NHC complexes have been ascribed to the greater relativistic effects of gold resulting from contraction of s and p orbitals while the d and f orbitals remain diffuse.[14a,28]

Further understanding of the NHC—M (M = Ag, Au) interaction was obtained by carrying out a detailed molecular orbital (MO) analysis using the AOMix-CDA software.[30] Specifically, the fragment orbital contributions from the free NHC ligands and the metal ion(s) to the frontier molecular orbitals in the (NHC)$_2$M$^+$Cl$^-$ type complexes (**1b**, **1c**, **2b**, **2c**), as well as in the 12-membered macrometallacycle [(NHC)$_2$M$_2$] type complexes (**3b**, **3c**, **4b**, **4c**), were examined. In particular, the contributions from the carbene lone pair of the free NHC ligands to the metal ion [C_{carb} → M (M = Ag, Au)] was closely examined as a part of our effort toward understanding the NHC—M interaction in these complexes.
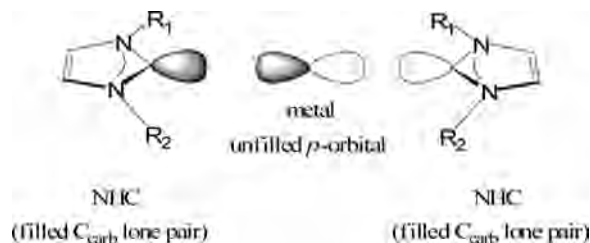
Figure 7. Interaction of filled carbene lone pair of NHC fragments with metal unfilled p orbital in the (NHC)$_2$M$^+$Cl$^-$ (M = Au, Ag) type **1b**, **1c**, **2b**, and **2c** complexes.

For the (NHC)$_2$M$^+$Cl$^-$ type complexes, **1b**, **1c**, **2b**, and **2c**, the C_{carb} → M (M = Ag, Au) donation is a part of a greater and more composite NHC—metal interaction (Supporting Information, Figures S6—S21), which consists of contributions from the different parts of the NHC ligand fragment to the metal center. Of the MOs related to the NHC—metal interaction, important is the MO depicting the C_{carb} → M donation, HOMO-7 (**1b**), HOMO-11 (**1c**), HOMO-9 (**2b**), HOMO-11 (**2c**), which contain a contribution from the carbene lone pair of the NHC ligand fragments to the unfilled p orbital of the metal ion fragment (Supporting Information, Figures S7, S9, S11, and S13). Specifically, the C_{carb} → M interaction involves approach of two carbene lone pairs of the NHC ligand fragments from the opposite directions to the unfilled p orbital of the metal ion at the center (Figure 7). Incidentally, the major contribution of the carbene lone pair of the NHC ligand fragment is seen to occur in these C_{carb} → M donation MOs. The other contributions from the NHC ligand fragment to the metal unfilled s orbitals that occur contain only a minor contribution from the carbene lone pair of the NHC ligand fragment (Supporting Information, Figures 6, S8, S10, and S12).

Similar to the {(NHC)$_2$M}$^+$Cl$^-$ complexes, for the 12-membered macrometallacyclic {(NHC)$_2$M$_2$} complexes too, the C_{carb} → M donation occur at multiple MOs of **3b**, **3c**, **4b**, and **4c** complexes and are part of a much larger and composite NHC—metal interaction, which contains contributions from different parts of the NHC ligand fragments. Furthermore, the MOs, HOMO-8 (**3b**), HOMO-9 (**3c**), HOMO-8 (**4b**), and HOMO-8 (**4c**), representing the major component of NHC → M (M = Ag, Au) donation, involve interactions between the carbene lone pair of the NHC ligand fragment with the unfilled s orbital of the metal ion fragment and rightfully depict the C_{carb} → M interaction (Supporting Information, Figures S15, S17, S19, S21). Thus, for the 12-membered {(NHC)$_2$M$_2$} type macrometallacycles, the C_{carb} → M interaction consists of the interaction between the carbene lone pair of the NHC ligand fragment with the unfilled s orbital of the metal ion (Figure 8). Hence, unlike what was observed in case of the [(NHC)$_2$M]$^+$Cl$^-$ type complexes, **1b**, **1c**, **2b**, and **2c**, where the carbene lone pair of the NHC fragments interacted with the unfilled metal p orbital (Figure 7), in the 12-membered macrometallacyclic [(NHC)$_2$M$_2$] type complexes, **3b**, **3c**, **4b**, and **4c**, the carbene lone pair interacted with the unfilled metal s orbital (Figure 8).

(30) Gorelsky, S. I. *AOMix: Program for Molecular Orbital Analysis*; York University: Toronto, Canada, 1997; http://www.sg-chem.net/ (accessed Mar 25, 2008).
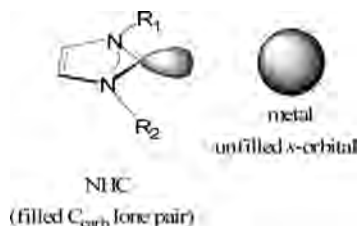
Figure 8. Interaction of filled carbene lone pair of NHC fragments with metal unfilled s orbital in 12-membered macrometallacyclic [(NHC)₂M₂] type **3b**, **3c**, **4b**, and **4c** complexes.

Table 3. Absorption and Emission Data for **1a**, **1b**, **1c**, **2a**, **2b**, **2c**, **3a**, **3b**, **3c**, **4a**, **4b**, and **4c**

compound	λ_{abs}, nm[a] (ε_{max} mm³ mol⁻¹ cm⁻¹)	room temperature		77 K
		λ_{em}, nm[b] in solid	λ_{em}, nm[a,b] in solution	λ_{em}, nm[c] in glassy solution
1a	243 (6000)	455	451	449
1b	242 (4300)	459	463	454
1c	244 (13000)	411	438	426
2a	243 (3900)	451	411	444
2b	243 (4500)	445	380	445
2c	245 (15000)	435	440	449
3a	244 (3600)	445	398	443
3b	243 (4000)	443, 635	442, 647	453, 580
3c	245 (10200)	442, 630	429, 623	449, 581
4a	243 (2800)	443	424	442
4b	243 (7000)	440, 632	435, 630	447, 591
4c	244 (17200)	446, 631	428, 627	446, 588

[a] Spectrum recorded in CHCl₃ at room temperature. [b] Excited at 264 nm. [c] Excited at 244 nm and the spectrum recorded in glassy solution of EtOH: MeOH (4: 1, v/v) mixture.
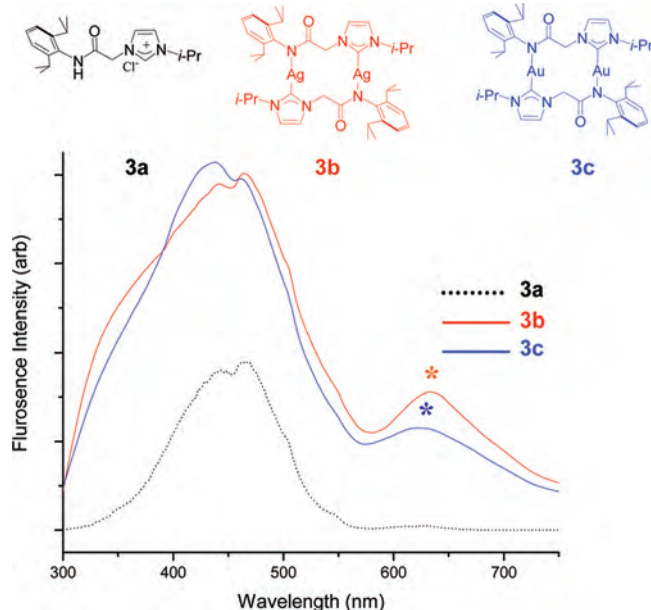
Figure 9. An overlay plot of the emission spectra of the ligand precursor **3a**, the silver complex **3b**, and the gold complex **3c** measured in the solid state at room temperature (excitation at 264 nm) is shown. The peak due to the tentative M···M (M = Ag and Au) interaction is marked by an * in the plot.

Photoluminescence Studies. To investigate the presence of any closed shell d¹⁰···d¹⁰ interaction in these silver and gold complexes, detailed photoluminescence studies were carried out (Table 3, Figures 9−11 and Supporting Information, Figures S22−S30). Specifically, the excitation wavelengths of these complexes were obtained from the respective electronic spectrum that showed an absorbance at about 243
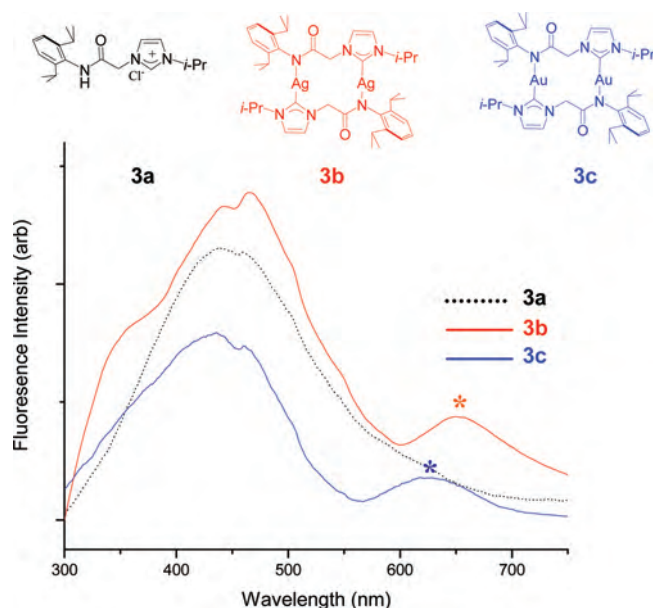
Figure 10. An overlay plot of the emission spectra of the ligand precursor **3a**, the silver complex **3b**, and the gold complex **3c** measured in chloroform (CHCl₃) at room temperature (excitation at 264 nm) is shown. The peak due to the tentative M···M (M = Ag and Au) interaction is marked by an * in the plot.
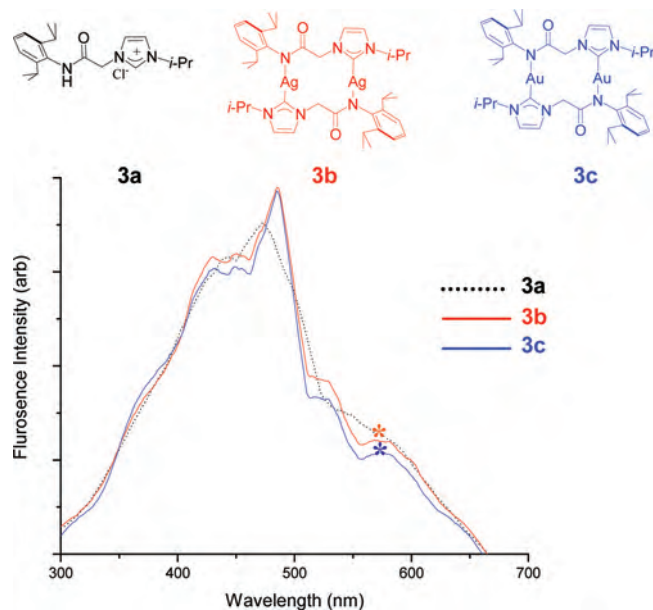
Figure 11. An overlay plot of the emission spectra of the ligand precursor **3a**, the silver complex **3b**, and the gold complex **3c** measured in a glassy solution of EtOH/MeOH (4: 1, v/v) mixture at low temperature (77 K; excitation at 244 nm) is shown. The peak due to the tentative M···M (M = Ag and Au) interaction is marked by an * in the plot.

nm, assigned to be a ligand based transition, as the ligand carbene precursors showed absorbances in the same region (**1a**, 243 nm; **2a**, 243 nm; **3a**, 244 nm; **4a**, 243 nm). The corresponding emission spectrum of these metal complexes showed a strong band at about the 380−463 nm region, which has also been assigned as an inter ligand transition based on the emission from the respective ligand carbene precursors (Table 3, Figures 9−11 and Supporting Information, Figures S22−S30). Quite interestingly, an additional low energy band was observed in the macrometallacyclic **3b**, **3c**, **4b**, and **4c** complexes, both in the solid state and in

solution at room temperature and at low temperature (77 K); this has been tentatively assigned to that originating from a weak M···M (M = Ag, Au) interaction based on the comparison with the respective imidazolium chloride ligand precursors (Table 3, Figures 9−11 and Supporting Information, Figures S22−S30). However, detailed theoretical studies are needed for unambiguous assignment of the emission because of the M···M (M = Ag, Au) interaction as the M···M (M = Ag, Au) contacts in both the *chair* and *boat* conformations of the **3b**, **3c**, **4b**, and **4c** complexes are greater than twice the van der Waals radii of the respective metals (Ag = 3.44 Å, Au = 3.32 Å).[23] It is worth noting that the metallophilic interaction, being attractive in nature, may be naturally present at the 3.403–3.985 Å M···M (M = Ag, Au) contact distances seen in **3b**, **3c**, **4b**, and **4c** but in much subdued form. In this regard, it is also worth mentioning that in a pair of dimeric {(NHC)MCl}$_2$ (M = Ag, A,u) complexes,[31] which exhibited much shorter M···M contact [d(Ag···Ag) = 3.1970(12) Å, d(Au···Au) = 3.2042(2) Å], the emission peak due to the M···M interaction appeared at much higher energy [527 nm for Ag, 529 nm for Au] compared to the macrometallacyclic **3b**, **3c**, **4b**, and **4c** complexes, which exhibited much longer M···M contacts [3.403–3.985 Å] and consequently much lower emissions (580–647 nm), implying the presence of weaker M···M interactions in the **3b**, **3c**, **4b**, and **4c** complexes. Similar low energy emissions at about 600 nm attributable to the Au···Au interaction have been observed earlier in Au−NHC complexes. For example, the [1,3-(*di*methyl)benzimidazol-2-ylidene]AuCl[32] and [1,3-(*di*methyl)imidazol-2-ylidene]-AuCl[33] complexes showed low energy emission attributed to the Au···Au interaction at 620 and 650 nm, respectively.

Conclusion

In summary, a series of structurally diverse silver and gold complexes of amido-functionalized N-heterocyclic carbenes ranging from ionic (NHC)$_2$M$^+$Cl$^-$ (M = Ag, Au; **1b**, **1c**, **2b**, **2c**) type to 12-membered macrometallacyclic {(NHC)$_2$-M$_2$} (M = Ag, Au; **3b**, **3c**, **4b**, **4c**) type complexes have been synthesized employing a common synthetic route whereby the structural diversity in these complexes has been achieved by a mere substituent effect. The nature of the NHC-metal bonding has been probed by DFT studies that revealed that the NHCs are good σ-donating ligands with relatively weaker π-accepting properties. The electron donation from the carbene lone pair of the N-heterocyclic carbene ligand, that is, the C$_{carb}$ → M (M = Ag, Au) donation, occurred primarily at an unfilled p orbital of the metal (5p for Ag and 6p for Au) for the ionic **1b**, **1c**, **2b**, and **2c** complexes and at the unfilled s orbital of the metal (5s for Ag and 6s for Au) for the macrometallacyclic **3b**, **3c**, **4b**, and **4c** complexes. The NHC−Au bond energies are signifi-

cantly greater than the corresponding NHC−Ag bond energies, giving credence to the transmetalation reaction of Ag−NHC complexes employed in synthesizing the Au−NHC complexes. Furthermore, the low energy emission band (580–647 nm) exhibited by the macrometallacyclic **3b**, **3c**, **4b**, and **4c** complexes in the photoluminescence study suggest the presence of weak metallophilic interaction in these complexes.

Experimental Section

General Procedures. All manipulations were carried out using a combination of a glovebox and standard Schlenk techniques. Solvents were purified and degassed by standard procedures. Ag$_2$O was purchased from SD-fine Chemicals (India) and used without any further purification. 1-*i*-propylimidazole,[34] 1-*t*-butylimidazole,[34] *N*-(*t*-butylchloroacetamide),[35] and *N*-(2,6-di*i*-propylphenylchloro-acetamide)[35] were synthesized according to literature procedures. ^{1}H and ^{13}C{^{1}H} NMR spectra were recorded on a Varian 400 MHz NMR spectrometer. ^{1}H NMR peaks are labeled as singlet (s), doublet (d), triplet (t), and septet (sept). Infrared spectra were recorded on a Perkin-Elmer Spectrum One FT-IR spectrometer. Mass spectrometry measurements were done on a Micromass Q-Tof spectrometer. Absorption and fluorescence spectra are recorded on a JASCO V570 spectrophotometer and Perkin-Elmer LS55 spectrofluorimeter.

Synthesis of 1-(*i*-Propyl)-3-{*N*-(*t*-butylacetamido)}imidazo-lium Chloride (1a). A mixture of *N*-*t*-butylchloroacetamide (0.694 g, 4.66 mmol) and 1-*i*-propylimidazole (0.513 g, 4.66 mmol) were taken in toluene (ca. 20 mL) and refluxed for 12 h, during which a brown precipitate was formed. The precipitate was isolated by decanting off the solvent, washed with hot hexane (ca. 20 mL), and dried under vacuum to give the product **1a** as a brown solid (0.873 g, 72%). ^{1}H NMR (CDCl$_3$, 400 MHz, 25 °C), δ 9.97 (s, 1H, NC*H*N), 8.66 (s, 1H, N*H*), 7.63 (s, 1H, NCHC*H*N), 7.30 (s, 1H, NC*H*CHN), 5.32 (s, 2H, C*H$_2$*), 4.75 (sept, 1H, $^3J_{HH}$ = 7 Hz, C*H*(CH$_3$)$_2$), 1.62 (d, 6H, $^3J_{HH}$ = 7 Hz, CH(C*H$_3$*)$_2$), 1.38 (s, 9H, (C*H$_3$*)$_3$). ^{13}C{^{1}H} NMR (CDCl$_3$, 100 MHz, 25 °C), δ 163.1 (*C*=O) 135.0 (N*C*HN), 122.9 (N*C*HCHN), 119.0 (NCH*C*HN), 52.4 (*C*H$_2$), 51.2 (*C*(CH$_3$)$_3$), 51.1 (*C*H(CH$_3$)$_2$), 27.7 (C(*C*H$_3$)$_3$), 22.2 (CH(*C*H$_3$)$_2$). IR (KBr pellet): 1674 (s) (ν_{CONH}). LRMS (ES): *m/z* 224 [(NHC)]$^+$ 100%. HRMS (ES): *m/z* 224.1754 [(NHC-ligand)]$^+$. Calcd 224.1763.

Synthesis of [1-(*i*-Propyl)-3-{*N*-(*t*-butylacetamido)imidazol-2-ylidene}]$_2$Ag$^+$Cl$^-$ (1b). A mixture of 1-(*i*-propyl)-3-{*N*-(*t*-butylacetamido)}imidazolium chloride (0.738 g, 2.84 mmol) and Ag$_2$O (0.329 g, 1.42 mmol) in dichloromethane (ca. 45 mL) was stirred for 4 h at room temperature. The reaction mixture was filtered, and the filtrate was dried under vacuum to give the product **1b** as a light yellow solid (0.596 g, 71%). ^{1}H NMR (CDCl$_3$, 400 MHz, 25 °C), δ 7.65 (br, 1H, N*H*), 7.33 (s, 1H, NC*H*CHN), 7.01 (s, 1H, NCHC*H*N), 5.07 (s, 2H, C*H$_2$*), 4.70 (sept, 1H, $^3J_{HH}$ = 7 Hz, C*H*(CH$_3$)$_2$), 1.48 (d, 6H, $^3J_{HH}$ = 7 Hz, CH(C*H$_3$*)$_2$), 1.37 (s, 9H, (C*H$_3$*)$_3$). ^{13}C{^{1}H} NMR (CDCl$_3$, 100 MHz, 25 °C), δ 179.7 (N*C*N), 165.9 (*C*=O), 122.8 (N*C*HCHN), 116.3 (NCH*C*HN), 54.2 (*C*H$_2$), 53.6 (*C*(CH$_3$)$_3$), 51.1 (*C*H(CH$_3$)$_2$), 28.3 (C(*C*H$_3$)$_3$), 23.4 (CH(*C*H$_3$)$_2$). IR (KBr pellet): 1674 (s) (ν_{CONH}). LRMS (ES): *m/z*

(31) (a) Ray, L.; Shaikh, M. M.; Ghosh, P. *Inorg. Chem.* **2008**, *47*, 230−240.

(32) Wang, H. M. J.; Chen, C. Y. L.; Lin, I. J. B. *Organometallics* **1999**, *18*, 1216–1223.

(33) Wang, H. M. J.; Vasam, C. S.; Tsai, T. Y. R.; Chen, S.-H.; Chang, A. H. H.; Lin, I. J. B. *Organometallics* **2005**, *24*, 486–493.

(34) Mas-Marzà, E.; Peris, E.; Castro-Ròdaiguez, I.; Meyer, K. *Organo-metallics* **2005**, *24*, 3158–3162.

(35) Dave, M. P.; Patel, J. M.; Langalia, N. A.; Shah, S. R.; Thaker, K. A. *J. Indian Chem. Soc.* **1985**, *LXII*, 386–387.

555 [(NHC)₂Ag⁺ 100%]. Anal. Calcd for C₂₄H₄₂AgClN₆O₂·(CH₂Cl₂): C, 44.49; H, 6.57; N, 12.45. Found: C, 44.83; H, 6.90; N, 12.69.

Synthesis of [1-(*i*-Propyl)-3-{*N*-(*t*-butylacetamido)imidazol-2-ylidene}]₂Au⁺Cl⁻ (1c). A mixture of [1-(*i*-propyl)-3-{*N*-(*t*-butylacetamido)imidazol-2-ylidene}]₂Ag⁺Cl⁻ (0.101 g, 0.171 mmol) and (SMe₂)AuCl (0.051 g, 0.171 mmol) in dichloromethane (ca. 30 mL) was stirred at room temperature for 4 h, at which point the formation of an off-white AgCl precipitate was observed. The reaction mixture was filtered, and the filtrate was dried under vacuum to give the product **1c** as a white solid (0.076 g, 65%). ¹H NMR (CDCl₃, 400 MHz, 25 °C): δ 8.90 (s, 1H, N$\underline{H}$), 7.33 (s, 1H, NC$\underline{H}$CHN), 7.04 (s, 1H, NCHC$\underline{H}$N), 5.22 (s, 2H, C$\underline{H}_2$), 4.90 (sept, 1H, $^3J_{HH}$ = 7 Hz, C$\underline{H}$(CH₃)₂), 1.55 (d, 6H, $^3J_{HH}$ = 7 Hz, CH(C$\underline{H}_3$)₂), 1.36 (s, 9H, C(C$\underline{H}_3$)₃). ¹³C{¹H} NMR (CDCl₃, 100 MHz, 25 °C), δ 183.2 (N$\underline{C}$N), 165.7 ($\underline{C}$=O), 123.6 (N$\underline{C}$HCHN), 116.3 (NCH$\underline{C}$HN), 53.8 ($\underline{C}$H₂), 53.2 ($\underline{C}$(CH₃)₃), 51.4 ($\underline{C}$H(CH₃)₂), 28.4 (C($\underline{C}$H₃)₃), 23.3 (CH($\underline{C}$H₃)₂). IR (KBr pellet): 1683 (s) (ν_{CONH}). Anal. Calcd for C₂₄H₄₂AuClN₆O₂: C, 42.45; H, 6.23; N, 12.38. Found: C, 42.91; H, 6.11; N, 12.83.

Synthesis of 1-(*t*-Butyl)-3-{*N*-(*t*-butylacetamido)}imidazolium Chloride (2a). A mixture of *N*-*t*-butylchloroacetamide (1.74 g, 11.6 mmol) and 1-*t*-butylimidazole (1.44 g, 11.6 mmol) were taken in toluene (ca. 10 mL) and refluxed for 12 h during which a brown precipitate was formed. The precipitate was isolated by decanting off the solvent, washed with hot hexane (ca. 20 mL), and dried under vacuum to give the product **2a** as a brown sticky solid (2.34 g, 75%). ¹H NMR (CDCl₃, 400 MHz, 25 °C), δ 9.85 (s, 1H, NC$\underline{H}$N), 8.55 (s, 1H, N$\underline{H}$), 7.67 (s, 1H, NCHC$\underline{H}$N), 7.37 (s, 1H, NC$\underline{H}$CHN), 5.29 (s, 2H, C$\underline{H}_2$), 1.70 (s, 9H, C(C$\underline{H}_3$)₃), 1.37 (s, 9H, C(C$\underline{H}_3$)₃). ¹³C{¹H} NMR (CDCl₃, 100 MHz, 25 °C), δ 163.0 ($\underline{C}$=O), 134.6 (N$\underline{C}$HN), 122.7 (N$\underline{C}$HCHN), 118.5 (NCH$\underline{C}$HN), 59.2 ($\underline{C}$H₂), 51.2 ($\underline{C}$(CH₃)₃), 50.9 ($\underline{C}$(CH₃)₃), 29.0 (C($\underline{C}$H₃)₃), 27.6 (C($\underline{C}$H₃)₃). IR (KBr pellet): 1704 (s) (ν_{CONH}). LRMS (ES): *m/z* 238 [(NHC)]⁺ 100%. HRMS (ES): *m/z* 239.1990 [(NHC-ligand) + 1]⁺. Calcd 239.1998.

Synthesis of [1-(*t*-Butyl)-3-{*N*-(*t*-butylacetamido)imidazol-2-ylidene}]₂Ag⁺Cl⁻ (2b). A mixture of 1-(*t*-butyl)-3-{*N*-(*t*-butylacetamido)}imidazolium chloride (0.317 g, 1.16 mmol) and Ag₂O (0.134 g, 0.580 mmol) was stirred in dichloromethane (*ca.* 40 mL) for 4 h at room temperature. The reaction mixture was filtered, and the filtrate was dried under vacuum to give the product **2b** as a brown solid (0.247 g, 69%). ¹H NMR (CDCl₃, 400 MHz, 25 °C), δ 8.34 (s, 1H, N$\underline{H}$), 7.23 (s, 1H, NC$\underline{H}$CHN), 7.12 (s, 1H, NCHC$\underline{H}$N), 5.09 (s, 2H, C$\underline{H}_2$), 1.73 (s, 9H, C(C$\underline{H}_3$)₃), 1.34 (s, 9H, C(C$\underline{H}_3$)₃). ¹³C{¹H} NMR (CDCl₃, 100 MHz, 25 °C), δ 178.7 (N$\underline{C}$N), 165.7 ($\underline{C}$=O), 121.3 (N$\underline{C}$HCHN), 118.1 (NCH$\underline{C}$HN), 57.2 ($\underline{C}$H₂), 55.4 ($\underline{C}$(CH₃)₃), 51.2 ($\underline{C}$(CH₃)₃), 31.4 (C($\underline{C}$H₃)₃), 28.3 (C($\underline{C}$H₃)₃). IR (KBr pellet): 1671 (s) (ν_{CONH}). Anal. Calcd for C₂₆H₄₆AgClN₆O₂·(CH₂Cl₂): C, 46.13; H, 6.88; N, 11.96. Found: C, 45.91; H, 6.67; N, 11.85.

Synthesis of [1-(*t*-Butyl)-3-{*N*-(*t*-butylacetamido)imidazol-2-ylidene}]₂Au⁺Cl⁻ (2c). A mixture of [1-(*t*-butyl)-3-{*N*-(*t*-butylacetamido)imidazol-2-ylidene}]₂Ag]⁺Cl⁻ (0.108 g, 0.173 mmol) and (SMe₂)AuCl (0.051 g, 0.173 mmol) in dichloromethane (ca. 30 mL) was stirred at room temperature for 4 h, at which point the formation of an off-white AgCl precipitate was observed. The reaction mixture was filtered, and the filtrate was dried under vacuum to give the product **2c** as a white solid (0.081 g, 66%). ¹H NMR (CDCl₃, 400 MHz, 25 °C): δ 8.84 (s, 1H, N$\underline{H}$), 7.19 (s, 1H, NC$\underline{H}$CHN), 7.12 (s, 1H, NCHC$\underline{H}$N), 5.32 (s, 2H, C$\underline{H}_2$), 1.81 (s, 9H, C(C$\underline{H}_3$)₃), 1.34 (s, 9H, C(C$\underline{H}_3$)₃). ¹³C{¹H} NMR (CDCl₃, 100 MHz, 25 °C), δ 182.3 (N$\underline{C}$N), 165.5 ($\underline{C}$=O), 121.6

(N$\underline{C}$HCHN), 118.0 (NCH$\underline{C}$HN), 58.3 ($\underline{C}$H₂), 55.1 ($\underline{C}$(CH₃)₃), 51.3 ($\underline{C}$(CH₃)₃), 31.5 (C($\underline{C}$H₃)₃), 28.4 (C($\underline{C}$H₃)₃). LRMS (ES): *m/z* 672 [(NHC)₂Au⁺, 100%]. HRMS (ES): *m/z* 672.3415 [(NHC)₂Au]⁺. Calcd 672.3426. IR (KBr pellet): 1683 (s) (ν_{CONH}). Anal. Calcd for C₂₆H₄₆AuClN₆O₂: C, 44.16; H, 6.56; N, 11.89. Found: C, 44.35; H, 6.86; N. 12.37.

Synthesis of 1-(*i*-Propyl)-3-{*N*-(2,6-di*i*-propylphenylacetamido)}-imidazolium Chloride (3a). A mixture of *N*-(2,6-di*i*-propylphenylchloroacetamide) (2.14 g, 8.46 mmol) and 1-*i*-propylimidazole (1.07 g, 9.73 mmol) were taken in toluene (ca. 15 mL) and was refluxed for 12 h during which a brown precipitate was formed. The precipitate was isolated by decanting off the solvent, washed with hot hexane (ca.20 mL), and dried under vacuum to give product **3a** as a brown sticky solid (2.43 g, 79%). ¹H NMR (CDCl₃, 400 MHz, 25 °C), δ 10.52 (s, 1H, N$\underline{H}$), 10.14 (s, 1H, NC$\underline{H}$N), 7.77 (s, 1H, NC$\underline{H}$CHN), 7.27 (s, 1H, NCHC$\underline{H}$N), 7.24–7.12 (m, 3H, C₆$\underline{H}_3${2,6-i-Pr₂}), 5.63 (s, 2H, C$\underline{H}_2$), 4.69 (sept, 1H, $^3J_{HH}$ = 7 Hz, C$\underline{H}$(CH₃)₂), 3.05 (sept, 1H, $^3J_{HH}$ = 7 Hz, C$\underline{H}$(CH₃)₂), 1.58 (d, 6H, $^3J_{HH}$ = 7 Hz, CH(C$\underline{H}_3$)₂), 1.13 (br, 12H, CH(C$\underline{H}_3$)₂). ¹³C{¹H} NMR (CDCl₃, 100 MHz, 25 °C), δ 164.3 ($\underline{C}$=O), 145.7 (N$\underline{C}$HN), 135.5 (*ipso*-$\underline{C}_6$H₃{2,6-i-Pr₂}), 130.7 (*o*-$\underline{C}_6$H₃{2,6-i-Pr₂}), 127.9 (*p*-$\underline{C}_6$H₃{2,6-i-Pr₂}), 123.3 (N$\underline{C}$HCHN), 122.9 (NCH$\underline{C}$HN), 119.4 (*m*-$\underline{C}_6$H₃{2,6-i-Pr₂}), 52.9 ($\underline{C}$H₂), 51.3 ($\underline{C}$H(CH₃)₂), 28.3 ($\underline{C}$H(CH₃)₂), 23.5 (CH($\underline{C}$H₃)₂), 22.6 (CH($\underline{C}$H₃)₂). IR (KBr pellet): 1692 (s) (ν_{CONH}). LRMS (ES): *m/z* 328 [(NHC)]⁺ 100%. HRMS (ES): *m/z* 328.2383 [(NHC-ligand)]⁺. Calcd 328.2389.

Synthesis of [1-(*i*-Propyl)-3-{*N*-(2,6-di*i*-propylphenylacetamido)imidazol-2-ylidene}]₂Ag₂ (3b). A mixture of 1-(*i*-propyl)-3-{*N*-(2,6-di*i*-propylphenylacetamido)}imidazolium chloride (0.317 g, 0.873 mmol) and Ag₂O (0.242 g, 1.04 mmol) was stirred in dichloromethane (ca. 40 mL) for 4 h at room temperature. The reaction mixture was filtered, and the filtrate was dried under vacuum to give the product **3b** as a white solid (0.419 g, 55%). ¹H NMR (CDCl₃, 400 MHz, 25 °C), δ 7.55 (s, 2H, NC$\underline{H}$CHN), 7.06 (br, 6H, C₆$\underline{H}_3${2,6-i-Pr₂}), 6.95 (s, 2H, NCHC$\underline{H}$N), 4.96 (s, 4H, C$\underline{H}_2$), 4.28 (sept, 2H, $^3J_{HH}$ = 7 Hz, C$\underline{H}$(CH₃)₂), 3.17 (sept, 4H, $^3J_{HH}$ = 7 Hz, C$\underline{H}$(CH₃)₂), 1.31 (d, 12H, $^3J_{HH}$ = 7 Hz, CH(C$\underline{H}_3$)₂), 1.15 (d, 12H, $^3J_{HH}$ = 7 Hz, CH(C$\underline{H}_3$)₂), 1.05 (d, 12H, $^3J_{HH}$ = 7 Hz, CH(C$\underline{H}_3$)₂). ¹³C{¹H} NMR (CDCl₃, 100 MHz, 25 °C), δ 175.1 (N$\underline{C}$N), 169.0 ($\underline{C}$=O), 143.6 (*ipso*-$\underline{C}_6$H₃{2,6-i-Pr₂}), 142.4 (*o*-$\underline{C}_6$H₃{2,6-i-Pr₂}), 129.2 (*p*-$\underline{C}_6$H₃{2,6-i-Pr₂}), 124.4 (N$\underline{C}$HCHN), 122.8 (NCH$\underline{C}$HN), 116.8 (*m*-$\underline{C}_6$H₃{2,6-i-Pr₂}), 62.1 ($\underline{C}$H₂), 54.0 ($\underline{C}$H(CH₃)₂), 28.1 ($\underline{C}$H(CH₃)₂), 23.8 (CH($\underline{C}$H₃)₂) 23.6 (CH($\underline{C}$H₃)₂). IR (KBr pellet): 1692 (s) (ν_{CONH}). Anal. Calcd for C₄₀H₅₆Ag₂N₆O₂: C, 55.31; H, 6.50; N, 9.67. Found: C, 55.42; H, 6.44; N, 9.65.

Synthesis of [1-(*i*-Propyl)-3-{*N*-(2,6-di*i*-propylphenylacet-amido)imidazol-2-ylidene}]₂Au₂ (3c). A mixture of [1-(*i*-propyl)-3-{*N*-(2,6-di*i*-propylphenylacetamido)imidazol-2-ylidene}]₂Ag₂ (0.159 g, 0.182 mmol) and (SMe₂)AuCl (0.107 g, 0.364 mmol) in dichloromethane (ca. 30 mL) was stirred at room temperature for 4 h, at which point the formation of an off-white AgCl precipitate was observed. The reaction mixture was filtered, and the filtrate was dried under vacuum to give the product **3c** as a white solid (0.123 g, 65%). ¹H NMR (CDCl₃, 400 MHz, 25 °C): δ 7.58 (br, 2H, NC$\underline{H}$CHN), 7.12–7.09 (m, 6H, *p*- and *m*-C₆$\underline{H}_3${2,6-i-Pr₂}), 6.90 (br, 2H, NCHC$\underline{H}$N), 5.29 (s, 4H, C$\underline{H}_2$), 4.73 (sept, 2H, $^3J_{HH}$ = 7 Hz, C$\underline{H}$(CH₃)₂), 3.24 (sept, 4H, $^3J_{HH}$ = 7 Hz C$\underline{H}$(CH₃)₂), 1.36 (d, 12H, $^3J_{HH}$ = 7 Hz, CH(C$\underline{H}_3$)₂), 1.21 (d, 12H, $^3J_{HH}$ = 7 Hz, CH(C$\underline{H}_3$)₂), 1.02 (d, 12H, $^3J_{HH}$ = 7 Hz, CH(C$\underline{H}_3$)₂). ¹³C{¹H} NMR (CDCl₃, 100 MHz, 25 °C), δ 170.0 (N$\underline{C}$N), 167.5 ($\underline{C}$=O), 146.2 (*ipso*-$\underline{C}_6$H₃{2,6-i-Pr₂}), 143.4 (*o*-$\underline{C}_6$H₃{2,6-i-Pr₂}), 125.4 (*p*-$\underline{C}_6$H₃{2,6-i-Pr₂}), 123.4 (N$\underline{C}$HCHN), 122.9 (NCH$\underline{C}$HN), 116.1 (*m*-$\underline{C}_6$H₃{2,6-i-Pr₂}), 59.1 ($\underline{C}$H(CH₃)₂), 53.7 ($\underline{C}$H₂), 28.7 ($\underline{C}$H(CH₃)₂), 24.0

(CH(CH$_3$)$_2$), 23.3 (CH(CH$_3$)$_2$). IR (KBr pellet): 1711 (s) (ν_{CONH}). LRMS (ES): m/z 671 [{(NHC)$_2$Au$_2$ + Na + 2H} − {N−C$_6$H$_3$(2,6-i-Pr$_2$)COAu}]$^+$ 100%, 1047 {[(NHC)$_2$Au$_2$] + 1}$^+$ 20%. HRMS (ES): m/z 1047.3907 [(NHC-Au)$_2$]$^{2+}$. Calcd 1047.3874. Anal. Calcd for C$_{40}$H$_{56}$Au$_2$N$_6$O$_2$: C, 45.89; H, 5.39; N, 8.03. Found: C, 46.54; H, 5.15; N, 8.07.

Synthesis of 1-(*t*-Butyl)-3-{*N*-(2,6-di*i*-propylphenylacetamido)}-imidazolium chloride} (4a). A mixture of *N*-2,6-di*i*-propylphenylchloroacetamide (3.37 g, 13.3 mmol) and 1-*t*-butylimidazole (1.65 g, 13.3 mmol) were taken in toluene (ca. 15 mL) and refluxed for 12 h, during which a light brown precipitate was formed. The precipitate was isolated by decanting off the solvent, washed with hot hexane (ca.20 mL), and dried under vacuum to give the product **4a** as a brown sticky solid (3.99 g, 79%). ^{1}H NMR (CDCl$_3$, 400 MHz, 25 °C), δ 10.63 (s, 1H, NH), 10.18 (s, 1H, NCHN), 7.72 (s, 1H, NCHCHN), 7.46 (s, 1H, NCHCHN), 7.22 (t, 1H, $^3J_{HH}$ = 8 Hz, *p*-C$_6$$H_3${2,6-i-Pr$_2$}), 7.09 (d, 2H, $^3J_{HH}$ = 8 Hz, *m*-C$_6$$H_3${2,6-i-Pr$_2$}), 5.64 (s, 2H, C$H_2$), 3.05 (sept, 1H, $^3J_{HH}$ = 6 Hz, CH(CH$_3$)$_2$), 1.62 (s, 9H, C(CH_3)$_3$), 1.08 (s, 12H, $^3J_{HH}$ = 8 Hz, CH(CH_3)$_2$). ^{13}C{^{1}H} NMR (CDCl$_3$, 100 MHz, 25 °C), δ 164.3 (C=O), 145.5 (NCHN), 135.0 (*ipso*-C_6H$_3${2,6-i-Pr$_2$}), 130.7 (*o*-C_6H$_3${2,6-i-Pr$_2$}), 128.6 (*p*-C_6H$_3${2,6-i-Pr$_2$}), 123.2 (NCHCHN), 122.8 (NCHCHN), 119.0 (*m*-C_6H$_3${2,6-i-Pr$_2$}), 59.8 (CH$_2$), 51.4 (C(CH$_3$)$_3$), 30.2 (CH(CH$_3$)$_2$), 29.3 (C(CH$_3$)$_3$), 28.2 (CH(CH$_3$)$_2$). IR (KBr pellet): 1696 (s) (ν_{CONH}). LRMS (ES): m/z 342 [(NHC)]$^+$ 100%. HRMS (ES): m/z 342.2556 [(NHC-ligand)]$^+$. Calcd 342.2545.

Synthesis of [1-(*t*-Butyl)-3-{*N*-(2,6-di*i*-propylphenylacetamido)imidazol-2-ylidene}]$_2$Ag$_2$ (4b). A mixture of 1-(*t*-butyl)-3-{*N*-(2,6-di*i*-propylphenylacetamido)}imidazolium chloride (0.359 g, 0.952 mmol) and Ag$_2$O (0.274 g, 1.19 mmol) was stirred in dichloromethane (ca. 40 mL) for 4 h at room temperature. The reaction mixture was filtered, and the filtrate was dried under vacuum to give the product **4b** as a light gray solid (0.425 g, 50%). ^{1}H NMR (CDCl$_3$, 400 MHz, 25 °C): δ 7.55 (s, 2H, NCHCHN), 7.06 (s, 2H, NCHCHN), 7.03 (br, 6H, C$_6$$H_3${2,6-i-Pr$_2$}), 5.10 (s, 4H, C$H_2$), 3.15 (sept, 4H, $^3J_{HH}$ = 7 Hz, CH(CH$_2$)$_2$), 1.36 (s, 18H, (CH_3)$_3$), 1.10 (d, 12H, $^3J_{HH}$ = 7 Hz, CH(CH_3)$_2$), 1.01 (d, 12H, $^3J_{HH}$ = 7 Hz, CH(CH_3)$_2$). ^{13}C{^{1}H} NMR (CDCl$_3$, 100 MHz, 25 °C), δ 173.8 (NCN), 168.9 (C=O), 144.0 (*ipso*-C_6H$_3${2,6-i-Pr$_2$}), 142.2 (*m*-C_6H$_3${2,6-i-Pr$_2$}), 124.3 (*p*-C_6H$_3${2,6-i-Pr$_2$}), 122.7 (NCHCHN), 120.6 (NCHCHN), 118.5 (*m*-C_6H$_3${2,6-i-Pr$_2$}), 63.2 (CH$_2$), 57.1 (C(CH$_3$)$_3$), 31.3 (CH(CH$_3$)$_2$), 28.1 (C(CH$_3$)$_3$), 24.2 (CH(CH$_3$)$_2$), 23.3 (CH(CH$_3$)$_2$). IR (KBr pellet): 1693 (s) (ν_{CONH}). Anal. Calcd for C$_{42}$H$_{60}$Ag$_2$N$_6$O$_2$: C, 56.26; H, 6.74; N, 9.37. Found: C, 56.33; H, 7.50; N, 8.98.

Synthesis of [1-(*t*-Butyl)-3-{*N*-(2,6-di*i*-propylphenylacetamido)imidazol-2-ylidene}]$_2$Au$_2$ (4c). A mixture of [1-(*t*-butyl)-3-{*N*-(2,6-di*i*-propylphenylacetamido)imidazol-2-ylidene}]$_2$Ag$_2$ (0.501 g, 0.560 mmol) and (SMe$_2$)AuCl (0.339 g, 1.14 mmol) in dichloromethane (ca. 75 mL) was stirred at room temperature for 4 h, at which point the formation of an off-white AgCl precipitate was observed. The reaction mixture was filtered and the filtrate was dried under vacuum to give the product **4c** as a white solid (0.429 g, 71%). ^{1}H NMR (CDCl$_3$, 400 MHz, 25 °C): δ 7.60 (s, 2H, NCHCHN), 7.26 (s, 2H, NCHCHN), 7.09–7.01 (m, 6H, C$_6$$H_3${2,6-i-Pr$_2$}), 5.48 (s, 4H, C$H_2$), 3.33 (sept, 2H, $^3J_{HH}$ = 6 Hz CH(CH$_3$)$_2$), 1.50 (s, 18H, (CH_3)$_3$), 1.15 (d, 12H, $^3J_{HH}$ = 6 Hz, CH(CH_3)$_2$), 0.983 (d, 12H, $^3J_{HH}$ = 6 Hz, CH(CH_3)$_2$). ^{13}C{^{1}H} NMR (CDCl$_3$, 100 MHz, 25 °C), δ 169.7 (NCN), 167.5 (C=O), 143.1 (*ipso*-C_6H$_3${2,6-i-Pr$_2$}), 142.8 (*o*-C_6H$_3${2,6-i-Pr$_2$}), 125.3 (*p*-C_6H$_3${2,6-i-Pr$_2$}), 122.8 (NCHCHN), 120.4 (NCHCHN), 117.8 (*m*-C_6H$_3${2,6-i-Pr$_2$}), 59.9 (CH$_2$), 58.1 (C(CH$_3$)$_3$), 31.3 (CH(CH$_3$)$_2$), 27.8 (C(CH$_3$)$_3$), 24.3 (CH(CH$_3$)$_2$). IR (KBr pellet): 1672 (s) (ν_{CONH}). LRMS (ES): m/z

1075 {[(NHC)$_2$Au$_2$] + 1}$^+$ 100%, 538 {[(1/2(NHC)$_2$Au$_2$] + 1}$^+$ 30%. HRMS (ES): m/z 1075.4143 {[(NHC)$_2$Au$_2$] + 1}$^+$. Calcd 1075.4187. Anal. Calcd for C$_{42}$H$_{60}$Au$_2$N$_6$O$_2$: C, 46.93; H, 5.63; N, 7.82. Found: C, 46.62; H, 5.62; N, 8.30.

X-ray Structure Determination. X-ray diffraction data for compound **2b** was collected on a Bruker P4 diffractometer equipped with a SMART CCD detector, those of compounds **3b**, **3c**, and **4c** were collected on an Oxford diffraction XCALIBUR-S instrument, and those of **1b**, **1c**, **2c** and **4b** were collected on a Nonius Mach3 diffractometer (graphite-monochromatized Mo Kα radiation). The crystal data collection and refinement parameters are summarized in Tables 1 and 2. The structures were solved using direct methods and standard difference map techniques and were refined by full-matrix least-squares procedures on F^2 with SHELXTL (Version 6.10). The *t*-butyl group in structure **2b** exhibits 2-fold disorder and was modeled subject to the constraint of maintaining the carbon−carbon bond lengths to be equal.

Computational Methods. DFT calculations were performed on the silver and gold **1b**, **1c**, **2b**, **2c**, **3b**, **3c**, **4b**, and **4c** complexes using the GAUSSIAN 03[36] suite of quantum chemical programs. The Becke three parameter exchange functional in conjunction with the Lee–Yang–Parr correlation functional (B3LYP) has been employed in this study.[37,38] The Stuttgart−Dresden effective core potential (ECP), representing 19 core–electrons, along with valence basis sets (SDD) were used for silver[39] and gold.[40] All other atoms were treated with the 6–31G(d) basis set.[41]

Inspection of the metal–ligand donor–acceptor interactions was carried out using the charge decomposition analysis (CDA).[42] CDA is a valuable tool in analyzing the interactions between molecular fragments on a quantitative basis, with an emphasis on the electron donation.[43] The orbital contributions in the (NHC)$_2$M$^+$Cl$^-$ (M = Ag, Au) type complexes (**1b**, **1c**, **2b**, **2c**) and the 12-membered macrometallacycle [(NHC)$_2$M$_2$] type complexes (**3b**, **3c**, **4b**, **4c**), can be divided into three parts:

(i) σ-donation from the [NHC $\overset{\sigma}{\leftarrow}$ M] fragment

(ii) π-back-donation from the [NHC $\overset{\pi}{\leftarrow}$ M] fragment

(iii) a repulsive interaction arising between the occupied MOs of these two fragments.

The CDA calculations were performed using the program AOMix,[30] using the B3LYP/SDD, 6–31G(d) wave function. MO compositions and the overlap populations were calculated using the AOMix program.[30,44] The analysis of the MO compositions in terms of occupied and unoccupied fragment orbitals (OFOs and UFOs, respectively), construction of orbital interaction diagrams, and the charge decomposition analysis (CDA) were performed using

(36) Frisch, M. J. et al. *Gaussian 03*, Revision C.02. Gaussian Inc.: Wallingford, CT, 2004.

(37) Becke, A. D. *Phys. Rev. A* **1988**, *38*, 3098–3100.

(38) Lee, C.; Yang, W.; Parr, R. G. *Phys. Rev. B* **1988**, *38*, 785–789.

(39) (a) Dolg, M.; Wedig, U.; Stoll, H.; Preuss, H. *J. Chem. Phys.* **1987**, *86*, 866–872. (b) Andrae, D.; Häussermann, U.; Dolg, M.; Stoll, H.; Preuss, H. *Theor. Chim. Acta* **1990**, *77*, 123–141. (c) Alkauskas, A.; Baratoff, A.; Bruder, C. *J. Phys. Chem. A* **2004**, *108*, 6863–6868.

(40) (a) Wang, X.; Andrews, L. *J. Am. Chem. Soc.* **2001**, *123*, 12899–12900. (b) Faza, O. N.; Lopez, C. S.; Alvarez, R.; de Lera, A. R. *J. Am. Chem. Soc.* **2006**, *128*, 2434–2437.

(41) Hehre, W. J.; Ditchfield, R.; Pople, J. A. *J. Chem. Phys.* **1972**, *56*, 2257–2261.

(42) Dapprich, S.; Frenking, G. *J. Phys. Chem.* **1995**, *99*, 9352–9362.

(43) (a) Vyboishchikov, S. F.; Frenking, G. *Chem. Eur. J.* **1998**, *4*, 1439–1448. (b) Frenking, G.; Pidun, U. *J. Chem. Soc., Dalton Trans.* **1997**, 1653–1662.

(44) Gorelsky, S. I.; Lever, A. B. P. *J. Organomet. Chem.* **2001**, *635*, 187–196.

the AOMix-CDA program.[45] NBO analyses were performed using the NBO 3.1 program implemented in the GAUSSIAN03 package.[27]

(45) Gorelsky, S. I.; Ghosh, S.; Solomon, E. I. *J. Am. Chem. Soc.* **2006**, *128*, 278–290.

Supporting Information Available: CIF files giving crystallographic data for **1b**, **1c**, **2b**, **2c**, **3b**, **3c**, **4b**, and **4c**, and B3LYP single-point coordinates of **1b**, **1c**, **2b**, **2c**, **3b**, **3c**, **4b**, and **4c** (PDF). This material is available free of charge via the Internet at http://pubs.acs.org.

IC702186G